

Published in final edited form as:

*Neural Comput.* 2012 December ; 24(12): 3181–3190. doi:10.1162/NECO\_a\_00373.

## Tuning Low-Voltage-Activated A-Current for Silent Gain Modulation

**Ameera X. Patel**

Brain Mapping Unit, Department of Psychiatry, University of Cambridge, CB2 3EB, U.K.

**Naomi Murphy and Denis Burdakov**

Department of Pharmacology, University of Cambridge, CB2 1PD, U.K.

### Abstract

Modulation of stimulus-response gain and stability of spontaneous (unstimulated) firing are both important for neural computation. However, biologically plausible mechanisms that allow these distinct functional capabilities to coexist in the same neuron are poorly defined. Low-threshold, inactivating (A-type)  $K^+$  currents ( $I_A$ ) are found in many biological neurons and are historically known for enabling low-frequency firing. By performing simulations using a conductance-based model neuron, here we show that biologically plausible shifts in  $I_A$  conductance and inactivation kinetics produce dissociated effects on gain and intrinsic firing. This enables  $I_A$  to regulate gain without major changes in intrinsic firing rate. Tuning  $I_A$  properties may thus represent a previously unsuspected single-current mechanism of silent gain control in neurons.

### 1 Introduction

The ability of neurons to alter their gain, that is, to change the steepness of the relationship between input stimulus and output firing rate, is considered crucial for neural computation (Salinas & Thier, 2000; Salinas & Sejnowski, 2001). However, effective neural processing is also thought to rely on the ability to maintain stable electrical activity in the absence of stimuli (Turrigiano & Nelson, 2000; Davis & Bezprozvanny, 2001; Marder & Prinz, 2002). Thus, it is of interest to elucidate biologically feasible mechanisms that allow modulation of stimulus-response gain independently of intrinsic neuronal activity. Hitherto proposed mechanisms of achieving such “silent” gain modulation (i.e., changing stimulus responsiveness without changing neural activity in the absence of stimuli) rely on elaborate balancing of electrically opposite sets of synaptic inputs (Chance, Abbott, & Reyes, 2002) or somatic voltage-gated currents (Burdakov, 2005). While this can, in theory, achieve silent gain modulation, there is little evidence to suggest that such balanced changes in coincident and opposing sets of currents can be triggered by biologically relevant stimuli.

On the other hand, there is a large body of experimental evidence showing that endogenous stimuli (such as second messengers and neuromodulators) can tune the properties of individual voltage-gated currents. However, little is known about whether changes in a

single current can enable silent gain modulation. Here we have focused on a subthreshold current expressed in diverse types of neurons, the low-voltage-activated (LVA) transient A-type  $K^+$  current ( $I_A$ ) (Birnbaum et al., 2004). We explored the extent to which experimentally reported variations in LVA  $I_A$  properties can produce silent gain modulation.

## 2 Methods

To study the effects of  $I_A$  on neuronal gain, we used a previously published single-compartment, Hodgkin-Huxley-type model neuron that comprises an LVA  $I_A$ , six other membrane currents ( $I_{Na}$ ,  $I_{CaS}$ ,  $I_{KCa}$ ,  $I_{Kd}$ ,  $I_H$ , and  $I_{leak}$ ), and an intracellular calcium buffer (Prinz, Thirumalai, & Marder, 2003). All maximal conductances, channel kinetics, and reversal potentials ( $E_{rev}$ ) were as in the tonically firing model neuron in Prinz et al. (2003), except those for the LVA  $I_A$ , which were changed as indicated. The membrane area was constant at  $0.628 \times 10^{-3} \text{ cm}^2$  for all simulations. For simplicity of analysis, changes to parameters were constrained to keep the firing pattern tonic and regular and to avoid silence or bursts. Simulations were performed using Matlab stiff systems numerical integrator ode23s at a time resolution of  $25 \mu\text{s}$ .

Input-output gain was measured as the average gradient of the relationship between neuronal firing rate and driving current (as presented in Hz per nA) in the range of 0 to 0.4 nA driving current. In practice, this captured the steepest part of the tuning curve. The firing frequency plotted in these graphs was assessed 1 second after a change in the driving stimulus to avoid any confounding effects of adaptation.

We focused on two types of input stimulus: a sustained driving stimulus of variable intensity in the form of current, as occurs in a large class of biological neurons (Cowley et al., 2001; Burdakov et al., 2006) (see Figures 1 and 2), and a current-based synaptic input model (see Figure 3). The synaptic model was designed to introduce a series of impulses of 0.75 nA magnitude, each lasting 2 ms, at random intervals distributed by the Poisson distribution (see Figure 3A). The intensity of synaptic input was varied by changing the mean interpulse interval ( $\lambda$ ) between 1 and 30 ms.

## 3 Results

We examined three types of biologically plausible changes in LVA  $I_A$  properties. First, we varied  $I_A$  conductance ( $g_A$ ). Increasing  $g_A$  progressively reduced both the gain and the spontaneous firing rate (see Figures 1A–D). Given that the speed ( $\tau_h$ ) and voltage dependence of LVA  $I_A$  inactivation can vary in biological neurons (Lozovaya, Vulfius, Ilyin, & Krasts, 1993; Muller, Hallermann, & Swandulla, 1999; Burdakov & Ashcroft, 2002), we next examined the relationship between  $g_A$ , gain, and firing rate at (1) intermediate and voltage dependent  $\tau_h$  (from Prinz et al., 2003) (see Figure 1B); (2) slow voltage-independent  $\tau_h$  (150 ms) (see Figure 1C); and (3) fast voltage-independent  $\tau_h$  (25 ms) (see Figure 1D). Increasing  $g_A$  progressively reduced both gain and baseline unstimulated firing rate under all of these conditions. Thus,  $g_A$  can modulate gain, but this modulation is not entirely silent, as the spontaneous firing rate is also affected.

Second, we explored the effects of changes in the speed of  $I_A$  inactivation. For simplicity, in these simulations we made  $\tau_h$  voltage independent, as reported for some biological neurons (Burdakov & Ashcroft, 2002). Varying  $\tau_h$  within a biologically plausible range of values had little effect on our measure of gain or on tonic firing rate, irrespective of whether the  $V_{1/2}$  of inactivation was depolarized (see Figure 1E) or hyperpolarized (see Figure 1F).

Third, we varied the voltage dependence of  $I_A$  inactivation. Shifting the voltage at which inactivation is half-maximal ( $V_{1/2}$ ) toward positive potentials reduced both gain and baseline firing rate (see Figures 2B–2E; see Figure 2A for an example of how the neuron processed the same input for different values of  $V_{1/2}$ ). However, the changes in gain and intrinsic firing rate occurred at different ranges of  $V_{1/2}$ . In the hyperpolarized range ( $V_{1/2} < -75$  mV), as reported experimentally for some neuronal subtypes (Song et al., 1998; Starodub & Wood, 2000; Schone, Venner, Knowles, Karnani, & Burdakov, 2011), there were large effects on gain but not baseline firing (see Figures 2C–2E). This differential modulation of gain versus firing rate persisted at the three different types of  $\tau_h$ , as described above: (1) intermediate and voltage-dependent  $\tau_h$  (from Prinz et al., 2003) (see Figure 2C); (2) slow voltage-independent  $\tau_h$  (150 ms) (see Figure 2D); and (3) fast voltage-independent  $\tau_h$  (25 ms) (see Figure 2E). This suggests that changing the voltage dependence of  $I_A$  inactivation can lead to near-silent gain modulation regardless of the speed of inactivation within a biologically plausible range of inactivation  $V_{1/2}$  (see Figure 2A for an example of raw data).

To explore whether these findings hold true under a noisy input, as well as under sustained current inputs, as examined in Figures 1 and 2, we also simulated the effects of changing  $g_A$  and  $V_{1/2}$  of inactivation on firing driven by a fluctuating, synaptic-like, excitatory input (see Figure 3A and section 2). Similar to the simulations using a sustained driving input (see Figure 1), these simulations showed that increasing  $g_A$  progressively reduced both gain and baseline firing rate, but this was not entirely silent (see Figures 3B and 3C). On the other hand, again in concordance with the sustained-input simulations (see Figure 2), shifting the  $V_{1/2}$  of inactivation to more hyperpolarized potentials increased gain with little or no effect on baseline firing (see Figures 3D and 3E).

In view of these results, we next analyzed  $I_A$  current data in order to determine whether we could elucidate a mechanism of differential gain modulation. We measured the average  $I_A$  current per action potential, (averaged over 10 action potentials) under three physiological conditions:  $I_A$  inactivation  $V_{1/2}$  of  $-55$  mV (baseline),  $-80$  mV, and  $-105$  mV (see Figure 4A). We found that the relationship between average  $I_A$  current per spike and firing rate was considerably steeper for depolarized  $V_{1/2}$  than for hyperpolarized  $V_{1/2}$  (see Figure 4A). In contrast, the current-frequency relationship for  $I_H$  (an electrophysiological opponent of  $I_A$ ) was similarly steep for all three values of  $V_{1/2}$  (see Figure 4B). Thus, depolarizing shifts in inactivation  $V_{1/2}$  would affect high-frequency firing more than lower frequency firing. This would account for the silent-like gain modulation we observe in Figures 2A and 2B.

## 4 Discussion

Our results show that both  $g_A$  and  $I_A$  inactivation  $V_{1/2}$  are capable of modulating gain and intrinsic (baseline) firing differentially, to produce either non-silent ( $g_A$ ; see Figures 1A–

1D), or near-silent ( $V_{1/2}$  of inactivation; see Figure 2) gain modulation. These effects were consistent across a range of biologically plausible shifts in the voltage dependence and speed of inactivation (Lozovaya et al., 1993; Muller et al., 1999; Burdakov & Ashcroft, 2002), and also for two types of driving stimulus: a sustained current input, such as that triggered by certain neuromodulators (Cowley et al., 2001; Burdakov et al., 2006) (see Figures 1 and 2), and a fluctuating synaptic-like input (see Figure 3). We found  $\tau_h$  itself incapable of controlling the gain or baseline firing rate at either depolarized or hyperpolarized potentials (see Figures 1E and 1F). This suggests that while the speed of  $I_A$  inactivation presumably modulates temporal summation of phasic inputs, it modulates neither firing nor gain under the conditions studied here (tonic firing, tonic driving current).

We propose that the differential effects of changes in  $I_A$  parameters (demonstrated for inactivation  $V_{1/2}$ ) on gain versus intrinsic firing arise because the effects of  $I_A$  on firing depend on the average membrane potential of the neuron, which becomes more positive as the firing rate increases from a low (intrinsic) value to higher (stimulus-driven) values. Depolarizing  $I_A$   $V_{1/2}$  of inactivation affects the stimulus-driven (higher frequency) firing more than the intrinsic (lower frequency) firing (see Figure 4A). In our model, this steepening of the frequency dependence of  $I_A$  (see Figure 4A) was not accompanied by a corresponding steepening in its interspike opponent,  $I_H$  (see Figure 4B), showing that the kinetics of the two currents do not necessarily ensure coupled changes in their frequency dependencies.

We speculate that the  $I_A$   $V_{1/2}$  of inactivation could be more capable of silent gain modulation than  $g_A$  because these parameters cause different transformations in the  $I_A$  “permissive voltage window” (see Figure 4C). Shifts in  $g_A$  (1 in Figure 4C) will enhance  $I_A$  at all potentials at which it is active. However, shifts in the  $I_A$   $V_{1/2}$  of inactivation (2 in Figure 4C) would differentially enhance  $I_A$  at positive, but not negative, potentials because it moves the right-side (inactivation-set) boundary but not the left-side (activation-set) boundary of the  $I_A$  voltage window (see Figure 4C).

In summary, these results suggest that changes in  $I_A$  kinetics, especially in  $I_A$  inactivation  $V_{1/2}$ , can produce silent-like gain modulation without a requirement for any balancing changes in other currents. To the best of our knowledge, such a cellular mechanism of silent gain control has not previously been described. This mechanism is biologically plausible and could be of general physiological importance, especially considering that the LVA  $I_A$  is widely expressed in many biological neurons and that its voltage dependence of inactivation has been reported to be tunable by a number of neuromodulators (Lozovaya et al., 1993; Muller et al., 1999; Birnbaum et al., 2004).

## Acknowledgments

This work was supported by the ERC (FP7 grant to D. B.), the Wellcome Trust TMAT program, and the MB/PhD program at the University of Cambridge (PhD studentship to A.P.).

## References

Birnbaum SG, Varga AW, Yuan LL, Anderson AE, Sweatt JD, Schrader LA. Structure and function of Kv4-family transient potassium channels. *Physiol Rev.* 2004; 84:803–833. [PubMed: 15269337]

- Burdakov D. Gain control by concerted changes in IA and IH conductances. *Neural Comp.* 2005; 17:991–995.
- Burdakov D, Ashcroft FM. Cholecystokinin tunes firing of an electrically distinct subset of arcuate nucleus neurons by activating A-type potassium channels. *J Neurosci.* 2002; 22:6380–6387. [PubMed: 12151516]
- Burdakov D, Jensen LT, Alexopoulos H, Williams RH, Fearon IM, O’Kelly I, et al. Tandem-pore K<sup>+</sup> channels mediate inhibition of orexin neurons by glucose. *Neuron.* 2006; 50:711–722. [PubMed: 16731510]
- Chance FS, Abbott LF, Reyes AD. Gain modulation from background synaptic input. *Neuron.* 2002; 35:773–782. [PubMed: 12194875]
- Cowley MA, Smart JL, Rubinstein M, Cerdan MG, Diano S, Horvath TL, et al. Leptin activates anorexigenic POMC neurons through a neural network in the arcuate nucleus. *Nature.* 2001; 411:480–484. [PubMed: 11373681]
- Davis GW, Bezprozvanny I. Maintaining the stability of neural function: A homeostatic hypothesis. *Annu Rev Physiol.* 2001; 63:847–869. [PubMed: 11181978]
- Lozovaya NA, Vulfius CA, Ilyin VI, Krasts IV. Intracellular ATP modifies the voltage dependence of the fast transient outward K<sup>+</sup> current in *Lymnaea stagnalis* neurones. *J Physiol.* 1993; 464:441–455. [PubMed: 8229812]
- Marder E, Prinz AA. Modeling stability in neuron and network function: The role of activity in homeostasis. *Bioessays.* 2002; 24:1145–1154. [PubMed: 12447979]
- Muller W, Hallermann S, Swandulla D. Opioidergic modulation of voltage-activated K<sup>+</sup> currents in magnocellular neurons of the supraoptic nucleus in rat. *J Neurophysiol.* 1999; 81:1617–1625. [PubMed: 10200198]
- Prinz AA, Thirumalai V, Marder E. The functional consequences of changes in the strength and duration of synaptic inputs to oscillatory neurons. *J Neurosci.* 2003; 23:943–954. [PubMed: 12574423]
- Salinas E, Sejnowski TJ. Gain modulation in the central nervous system: Where behavior, neurophysiology, and computation meet. *Neuroscientist.* 2001; 7:430–440. [PubMed: 11597102]
- Salinas E, Thier P. Gain modulation: A major computational principle of the central nervous system. *Neuron.* 2000; 27:15–21. [PubMed: 10939327]
- Schone C, Venner A, Knowles D, Karnani MM, Burdakov D. Di-chotomous cellular properties of mouse orexin/hypocretin neurons. *J Physiol.* 2011; 589:2767–2779. [PubMed: 21486780]
- Song WJ, Tkatch T, Baranaukas G, Ichinohe N, Kitai ST, Surmeier DJ. Somatodendritic depolarization-activated potassium currents in rat neostriatal cholinergic interneurons are predominantly of the A type and attributable to coexpression of Kv4.2 and Kv4.1 subunits. *J Neurosci.* 1998; 18:3124–3137. [PubMed: 9547221]
- Starodub AM, Wood JD. A-type potassium current in myenteric neurons from guinea-pig small intestine. *Neuroscience.* 2000; 99:389–396. [PubMed: 10938445]
- Turrigiano GG, Nelson SB. Hebb and homeostasis in neuronal plasticity. *Curr Opin Neurobiol.* 2000; 10:358–364. [PubMed: 10851171]

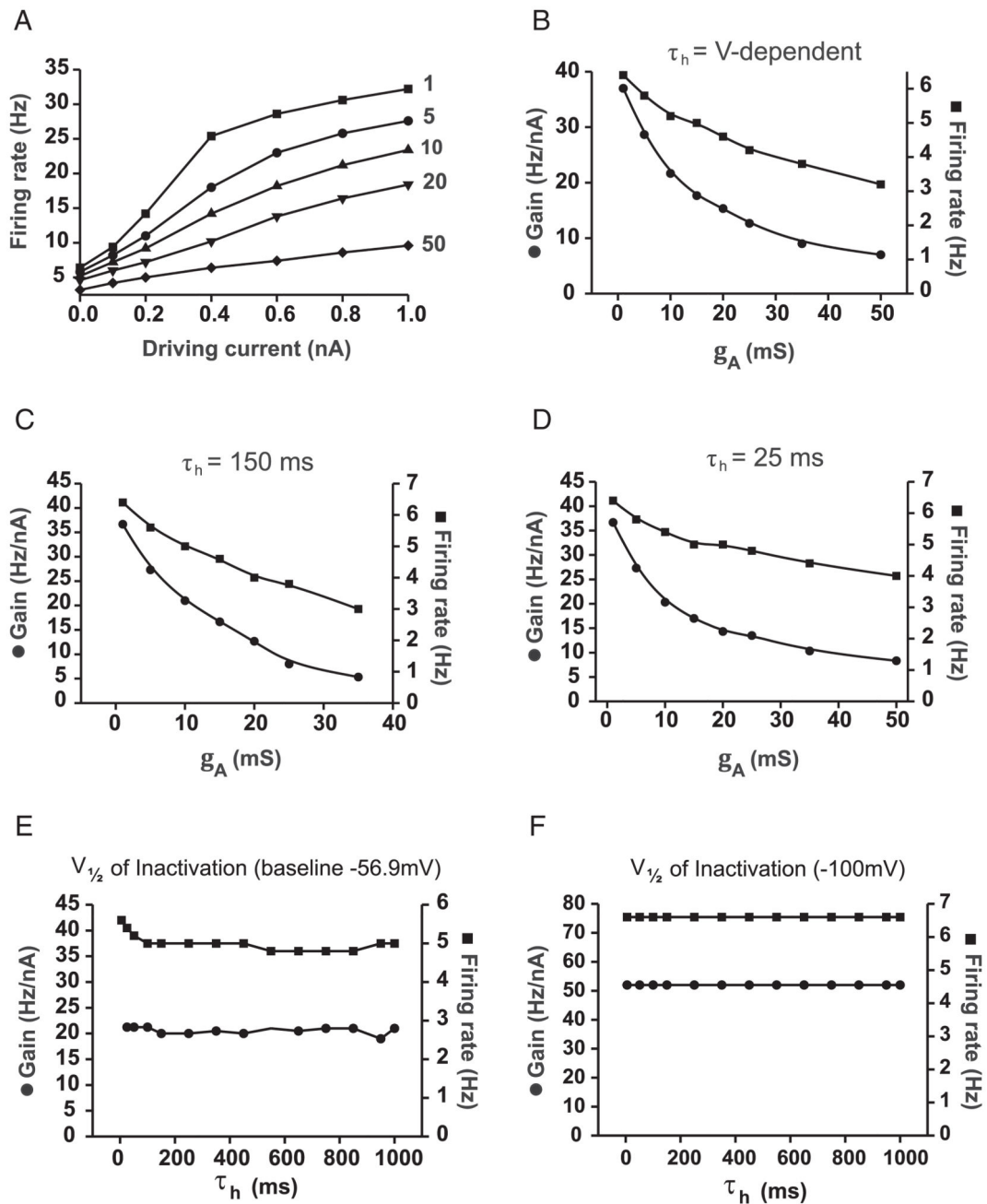


**Figure 1.**

(A) Input-output curves of the model neuron with different values of  $g_A$  (A-current conductance; values are given near corresponding datasets). (B) Relationship between  $g_A$  and gain (left  $y$ -axis) and between  $g_A$  and resting firing rate (right  $y$ -axis), where  $\tau_h$  is intermediate and voltage-dependent (as in Prinz et al., 2003). (C) Same as in panel B but with slow voltage-independent  $\tau_h$ (150 ms). (D) Same as in panel B, but with fast voltage-independent  $\tau_h$  (25 ms). (E) Relationship between  $\tau_h$  of inactivation and gain (left  $y$ -axis) and between  $\tau_h$  of inactivation and baseline firing rate (right  $y$ -axis), where  $\tau_h$  is voltage-

independent.  $V_{1/2}$  of inactivation is at baseline level ( $-56.9$  mV, as in Prinz et al., 2003). (F)  
Same plot as in panel E, but where  $V_{1/2}$  of inactivation is  $-100$  mV.

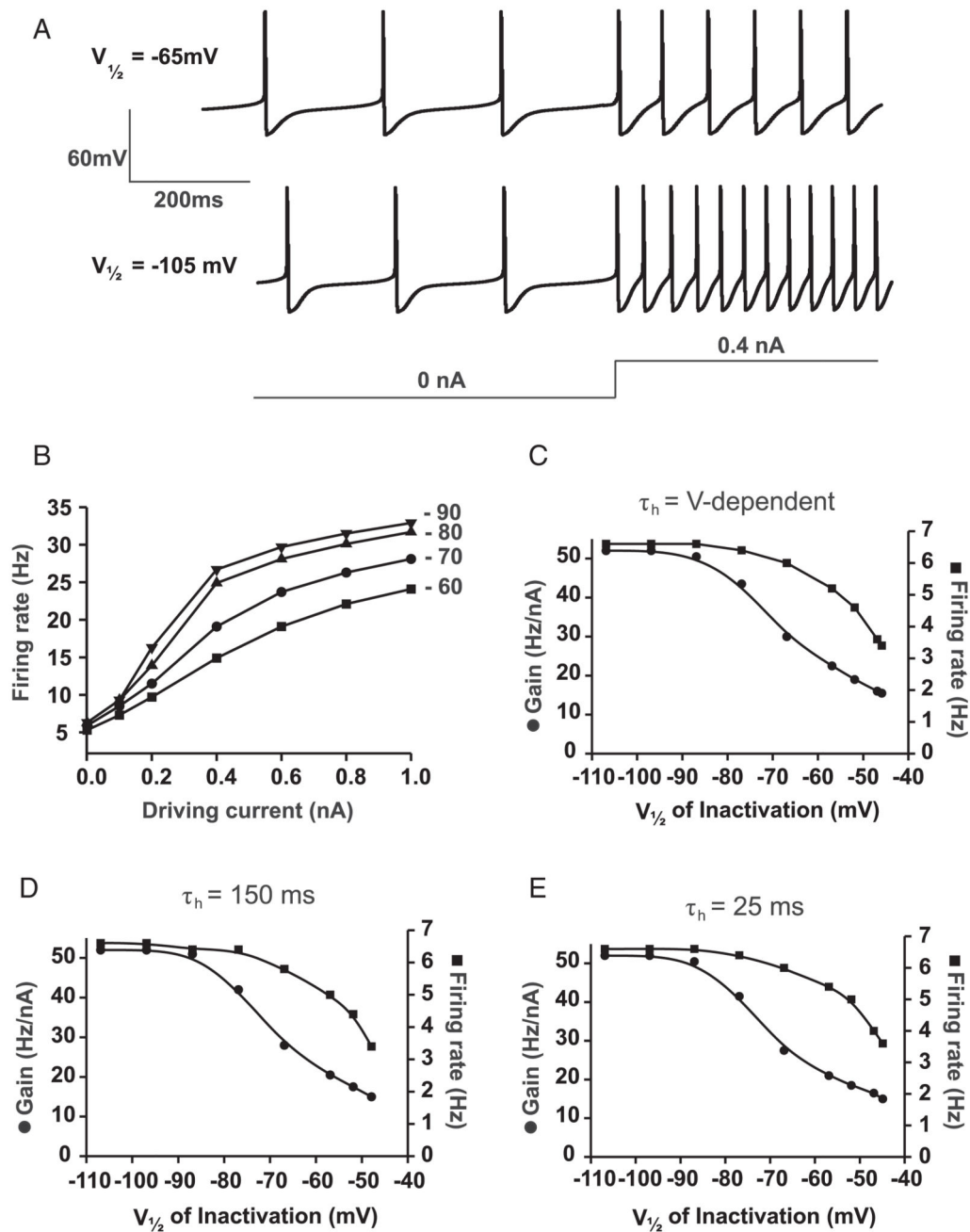


**Figure 2.**

(A) Examples of firing responses of the model neuron with different values of  $V_{1/2}$  of inactivation.  $\tau_h$  is intermediate and voltage-dependent. (B) Input-output relationships of the model neuron with different values of  $V_{1/2}$  of inactivation ( $V_{1/2}$  values given near corresponding datasets). (C) Relationship between  $V_{1/2}$  of inactivation and gain (left y-axis) and between  $V_{1/2}$  of inactivation and baseline firing rate (right y-axis), where  $\tau_h$  is intermediate and voltage-dependent (as in Prinz et al., 2003). (D) Same as in panel C, but

with slow voltage-independent  $\tau_h$  (150 ms). (E) Same as in panel C but with fast voltage-independent  $\tau_h$  (25 ms).

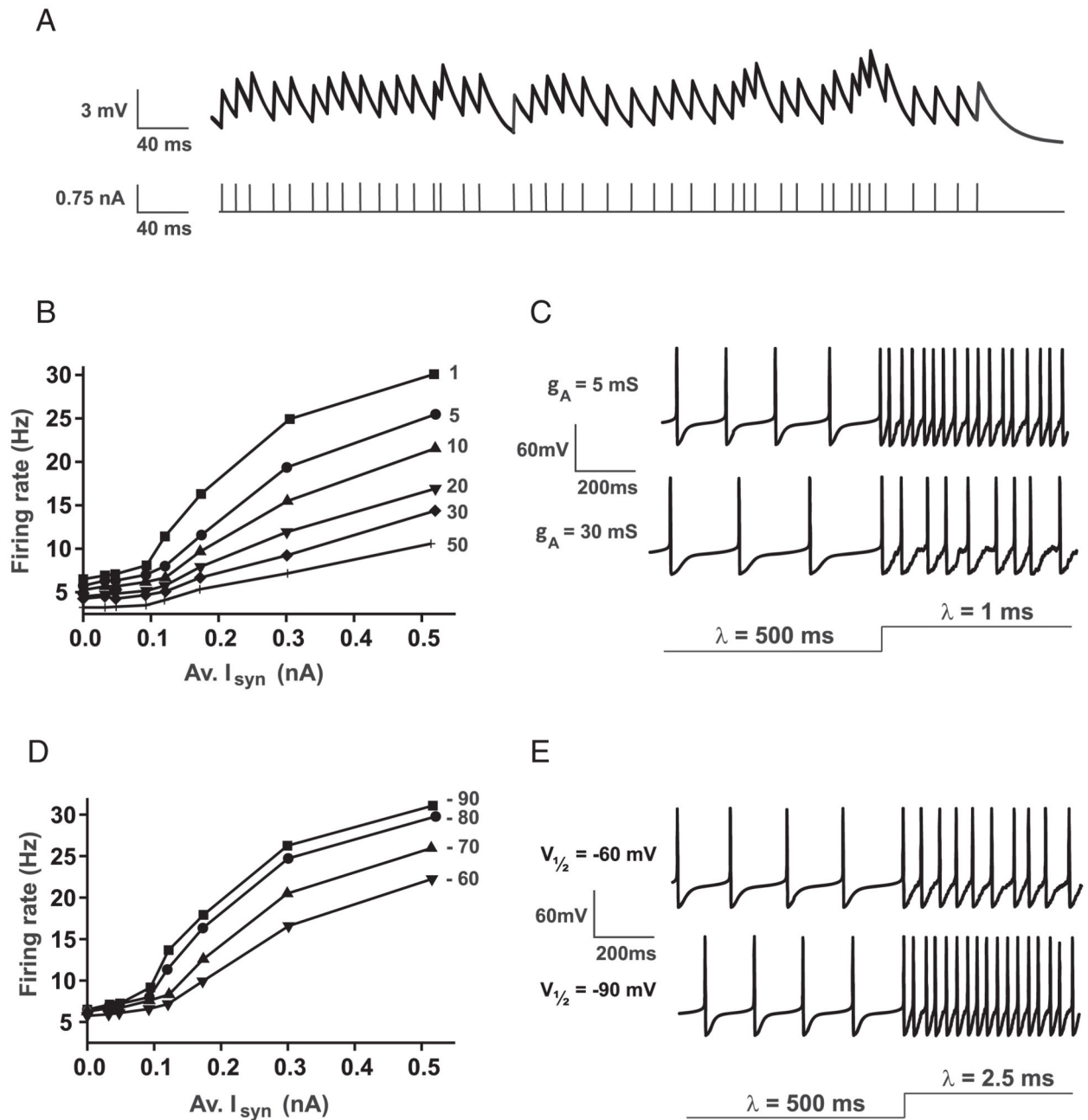


**Figure 3.**

(A) Example of noisy membrane potential generated by the synaptic model (upper trace) where impulses were generated by the Poisson distribution (lower trace) with a mean interimpulse interval of 20 ms. (B) Input-output relationships of the model neuron with different values of  $g_A$  ( $g_A$  values given near the corresponding dataset). Av.  $I_{syn}$  is the average synaptic current, which is driven by modulating the mean interimpulse interval ( $\lambda$ ) between 1 and 30 ms. (C) Examples of firing responses of the model neuron with different values of  $g_A$  using a model synaptic input (as demonstrated in panel A).  $g_A$  values are given

near the corresponding dataset.  $\lambda$  is the mean interval between impulses generated by the Poisson distribution. (D) Input-output relationships of the model neuron with different values of  $V_{1/2}$  of inactivation ( $V_{1/2}$  values given near corresponding datasets).  $\text{Av. } I_{\text{syn}}$  is the average synaptic current, which is again driven by changes in  $\lambda$ . (E) Examples of firing responses of the model neuron with different values of  $V_{1/2}$  of inactivation using the synaptic input model (as in panel C). Values of inactivation  $V_{1/2}$  are given near the corresponding dataset.  $\lambda$  is the mean interval between impulses, generated by the Poisson distribution.

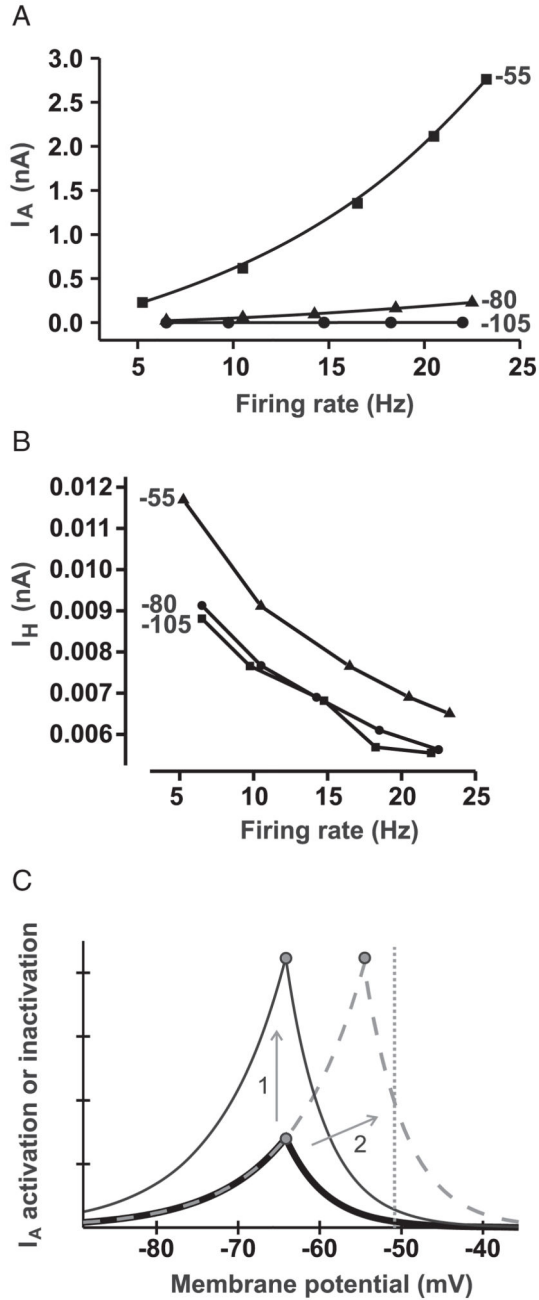


**Figure 4.**

(A) Relationship between average  $I_A$  current (averaged over 10 spikes) and firing rate. Values at end of curves are  $V_{1/2}$  of  $I_A$  used to generate those curves. (B) Same as in panel B, but for  $I_H$  (values near corresponding datasets are  $V_{1/2}$  of  $I_A$  values). (C) Schematic of permissive voltage window of  $I_A$ . Left sides of peaks are steady-state activation curves (m); right sides of peaks are steady-state inactivation curves (h). The complete m and h curves upward of the m-h intercepts (peaks) are not shown for visual clarity. The thick solid line is the control; the thin solid line represents increased  $g_A$ ; the dashed line represents

inactivation  $V_{1/2}$  shifted to positive potentials. The vertical dotted line shows the average membrane potential at the spontaneous firing rate ( $\sim 5$  Hz) of the model neuron.